Published online December 15, 2004

6490–6500 *Nucleic Acids Research, 2004, Vol. 32, No. 22*
doi:10.1093/nar/gkh987

Rad23 stabilizes Rad4 from degradation by the Ub/proteasome pathway

Tatiana G. Ortolan, Li Chen, Prasad Tongaonkar and Kiran Madura*

Department of Biochemistry, Robert Wood Johnson Medical School, 683 Hoes Lane, Piscataway, NJ 08854, USA

Received September 29, 2004; Revised and Accepted November 19, 2004

ABSTRACT

Rad23 protein interacts with the nucleotide excision-repair (NER) factor Rad4, and the dimer can bind damaged DNA. Rad23 also binds ubiquitinated proteins and promotes their degradation by the proteasome. Rad23/proteasome interaction is required for efficient NER, although the specific role of the Ub/proteasome system in DNA repair is unclear. We report that the availability of Rad4 contributes significantly to the cellular tolerance to UV light. Mutations in the proteasome, and in genes encoding the ubiquitin-conjugating enzymes Ubc4 and Ubc5, stabilized Rad4 and increased tolerance to UV light. A short amino acid sequence, previously identified in human Rad23, mediates the interaction between Rad23 and Rad4. We determined that this motif was required for stabilizing Rad4, and could function independently of the intact protein. A ubiquitin-like (UbL) domain in Rad23 binds the proteasome, and is required for conferring full resistance to DNA damage. However, Rad23/proteasome interaction appears unrelated to Rad23-mediated stabilization of Rad4. Specifically, simultaneous expression of a Rad23 mutant that could not bind the proteasome, with a mutant that could not interact with Rad4, fully suppressed the UV sensitivity of *rad23*Δ, demonstrating that Rad23 performs two independent, but concurrent roles in NER.

INTRODUCTION

Rad23 is a multi-domain and multi-functional protein that participates in DNA repair (1,2), stress response and cell-cycle control (3,4). Rad23 and related proteins that contain N-terminal ubiquitin-like (UbL) domains can bind the proteasome (5–8). Proteins with UbL domains often contain ubiquitin-associated (UBA) domains (9) that bind multi-ubiquitinated (multi-Ub) proteins (10–12). Cells that express a rad23 mutant that lacks the UbL domain are partly defective in nucleotide excision-repair (NER) (13), in contrast to a uba$^-$ mutant which is NER-proficient (10). A requirement for UbL/proteasome interaction was confirmed in a reconstituted DNA repair reaction (14).

Two distinct views concerning the role of the Ub/proteasome pathway in NER have emerged. A reconstituted system showed that Rad23/proteasome interaction, but not proteasome-mediated proteolysis, was required for efficient NER (14,15). In contrast, several studies showed that Rad23 promotes the degradation of ubiquitinated proteins by the proteasome (3,4,16–19). A further complication is suggested by evidence that Rad23 can stabilize the DNA repair factor Rad4 (20–25), which is contrasted by its well-defined function as a facilitator of proteolysis. The proteasome itself appears to have both positive and negative effects on NER. Despite a large body of work, it has been difficult to develop a coherent model that describes the link between NER and the Ub/proteasome system. One interpretation of these results is that Rad23 performs a non-proteolytic role in NER, which is distinct from its positive role in protein degradation in other pathways.

The purification of Rad4 (and its human ortholog XPC) is associated with co-purification of Rad23 (26,27). Rad4 and Rad23 (termed NEF2) function together in NER (28–31), although extensive investigation has not yielded insight into the biochemical function of Rad4. Because of their stoichiometric association, it was possible that Rad23 regulated Rad4 stability. Rad4 is a proteolytic substrate, since its levels increased in a proteasome mutant strain, and the protein was transiently stabilized following DNA damage (20). Furthermore, over-expression of Rad23 resulted in inhibition of Rad4 ubiquitination (20). Consistent with these results, high-level expression of Rad23 inhibited protein degradation (16,32–34). It is likely that Rad23 enables Rad4 to function in NER by protecting it from degradation by the proteasome (23,25). This scenario is not unusual, since free forms of subunits in multi-component complexes are often unstable, while their association with physiological partners can protect them (35). Conditional entrapment of Pds1 by Rad23 was also proposed to regulate its abundance (36). In line with this reasoning, mXPC levels were reduced in a mouse knockout of mHR23B (21).

The uncertainty of Rad23 function in NER has been partly resolved in recent studies, which showed that additional DNA repair proteins control Rad4 stability. Ramsey *et al*. (24) showed that Rad4 levels are regulated by Rad7 and Rad16 (NEF4), which encode a putative Ub (E3)-ligase. Genetic and biochemical associations among the NEF2 and NEF4 factors were previously reported (30,37,38). However, it remains to be determined how the NEF2 and NEF4 pathways control Rad4 abundance. Collectively, these findings suggest that several

*To whom correspondence should be addressed. Tel: +1 732 2350 5602; Fax: +1 732 235 4783; Email: maduraki@umdnj.edu

proteins in the NER pathway can regulate Rad4 abundance via the Ub/proteasome pathway. These recent findings validate long-standing genetic and biochemical connections between Rad23 and Rad7 (37,38).

We describe evidence here, which indicate that Rad23 participates in two distinct NER events. We determined that the interaction between Rad23 and Rad4 is critical for stabilizing Rad4, and that a small amino acid domain, previously recognized in human Rad23 (39,40) was sufficient for this interaction. The Rad4-binding (R4B) domain alone can stabilize Rad4, and promote NER in *rad23*Δ. Previous studies showed that loss of ubiquitin-conjugating enzyme Ubc4 could partially suppress the UV sensitivity of *rad23*Δ (32). The biochemical basis of this suppression is now understood, because we show here that Ubc4 and Ubc5 govern the stability of Rad4. Although Rad4 levels were reduced in *rad23*Δ, they were entirely restored in cells that also lacked Ubc4/Ubc5. These studies indicate that the levels of Rad4 have a strong bearing on cellular resistance to UV light. However, our genetic studies also indicated that Rad23 functioned in a separate, but concurrent activity in NER that involved interaction with the proteasome. This activity of Rad23 is distinct from its stabilization of Rad4. Remarkably, simultaneous expression of both mutant forms of rad23 protein restored full resistance to UV light.

MATERIALS AND METHODS

Strains

Table 1 lists the *Saccharomyces cerevisiae* strains used in this study. Chromosomal hemagglutinin (HA)-tagged *RAD4* was generated by homologous recombination (41). Plasmid pTO33 was constructed by cloning the BamHI–HindIII fragment from pDG65 (42), into YIplac211 (43), yielding an integrating plasmid that contained the *URA3* and *RAD4* genes. However, the coding sequence of Rad4 was interrupted by a 2.2 kb 'stuffer' sequence that was placed in the internal BglII restriction site (R. D. Gietz, University of Manitoba). A PCR-cloning strategy was used to insert a double HA tag just before the stop codon of the *RAD4* gene in pTO33, generating plasmid pTO34-2. pTO34-2 was digested with BglII to linearize the plasmid and remove the 'stuffer' sequence, and transformed into MHY501. Insertion of the linearized plasmid was selected on plates lacking uracil, while excision of the plasmid sequences, including the *URA3* gene, was counter-selected on medium containing 5-fluoroorotic acid and uracil. To delete the *RAD23* gene, we used pDG28 (R. D. Gietz, University of Manitoba), in which an internal 1.1 kb BglII fragment was replaced with the sequence encoding Ura3 (*rad23*Δ::*URA3*). Integrating plasmid pTO47, encoded Rad23 lacking residues 252–313 (rad23$^{\Delta R4B}$). The plasmid was linearized with MfeI and transformed into TOY95 cells.

Plasmids

Table 2 lists the plasmids used in this study. A 1.68 kb fragment, corresponding to the PpuMI-AccI chromosomal fragment containing *RAD23* gene was generated by PCR. The purified DNA fragment was cloned into YIplac211 as a BamHI–EcoRI fragment, to generate pTO35-2. Rad23 sequence coding for amino acids from 252 to 313 were cloned into pCBGST1, and expression induced with copper sulfate (44).

Table 1. Yeast strains

Strain	Genotype	Reference
CSY354	MHY501 *rad23Δ::URA3*	K. Madura
CSY403	CSY354, P_{CUP1}-*RAD4-HA LEU2* 2μ	K. Madura
CSY465	MHY501 *rad4Δ*	K. Madura
LCY 175	MHY501, P_{CUP1}-*RAD4-HA LEU2* 2μ	K. Madura
MHY498	MHY501 *ubc4-Δ1::HIS3*	(49)
MHY499	MHY501 *ubc5-Δ1::LEU2*	(49)
MHY501	*MATα his3-Δ200 leu2-3, 112 ura3-52 lys2-801 trp1-1*	(49)
MHY508	MHY501 *ubc4-Δ1::HIS3 ubc5-Δ1::LEU2*	(49)
Sc507	W303-1A *S10-SUG1*	(14)
Sc658	W303-1A *S10-sug1-20*	(15)
Sc660	W303-1A *S10-sug1-25*	(14)
TOY95	MHY501 *RAD4-HA*	This study
TOY103	TOY95 *rad23Δ::URA3*	This study
TOY116	TOY103, P_{CUP1}-*FLAG-RAD23 LEU2* 2μ	This study
TOY229	TOY95, P_{CUP1}-*GST TRP1* 2μ	This study
TOY230	TOY95, P_{CUP1}-*GST-R4B TRP1* 2μ	This study
TOY231	TOY95, P_{CUP1}-*GST-RAD23 TRP1* 2μ	This study
TOY232	TOY103, P_{CUP1}-*GST TRP1* 2μ	This study
TOY233	TOY103, P_{CUP1}-*GST-R4B TRP1* 2μ	This study
TOY234	TOY103, P_{CUP1}-*GST-RAD23 TRP1* 2μ	This study
TOY236	MHY498 *RAD4-HA rad23Δ::URA3*	This study
TOY239	MHY508 *RAD4-HA rad23Δ::URA3*	This study
TOY240	MHY499 *RAD4-HA rad23Δ::URA3*	This study
TOY268	MHY501 *rad23*$^{\Delta R4B}$	This study
TOY287	TOY103, P_{RAD23}-*RAD23 TRP1* 2μ	This study
TOY288	TOY103, P_{RAD23}-*rad23*$^{\Delta UbL}$ *TRP1* 2μ	This study
TOY289	TOY103, P_{RAD23}-*FLAG-RAD23 TRP1* 2μ	This study
TOY290	TOY103, P_{RAD23}-*rad23* $^{\Delta R4B}$ *TRP1* 2μ	This study
TOY291	TOY103, P_{RAD23}-*FLAG-rad23*$^{\Delta UbL}$ *TRP1* 2μ	This study
TOY292	TOY103, P_{RAD23}-*rad23*^{uba} *TRP1* 2μ	This study
TOY293	TOY103, P_{RAD23}-*FLAG-rad23*$^{\Delta R4B}$ *TRP1* 2μ	This study
TOY294	TOY103, P_{RAD23}-*FLAG-rad23*^{uba} *TRP1* 2μ	This study
TOY299	Sc507 *RAD4-HA rad23Δ::URA3*	This study
TOY300	Sc658 *RAD4-HA rad23Δ::URA3*	This study
TOY301	Sc660 *RAD4-HA rad23Δ::URA3*	This study
TOY319	TOY268, P_{RAD23}-*rad23*$^{\Delta UbL}$ *TRP1* 2μ	This study

Table 2. Plasmids used in this study

Plasmid	Description[a]	Reference
pCBGST1	P_{CUP1}-*GST TRP1* 2μ	(44)
pCS13	P_{CUP1}-*FLAG-RAD23 LEU2* 2μ	K. Madura (C. Schauber)
pKM1473	P_{CUP1}-*GST-RAD23 TRP1* 2μ	K. Madura
pTO41	P_{CUP1}-*GST-R4B TRP1* 2μ	This study
pTO47	P_{RAD23}-*FLAG-rad23*$^{\Delta R4B}$ *URA3*	This study
pTO61	P_{RAD23}-*RAD23 TRP1* 2μ	This study
pTO62	P_{RAD23}-*rad23*$^{\Delta UbL}$ *TRP1* 2μ	This study
pTO63	P_{RAD23}-*FLAG-RAD23 TRP1* 2μ	This study
pTO64	P_{RAD23}-*rad23* $^{\Delta R4B}$ *TRP1* 2μ	This study
pTO65	P_{RAD23}-*FLAG-rad23*$^{\Delta UbL}$ *TRP1* 2μ	This study
pTO66	P_{RAD23}-*rad23*^{uba} *TRP1* 2μ	This study
pTO67	P_{RAD23}-*FLAG-rad23*$^{\Delta R4B}$ *TRP1* 2μ	This study
pTO68	P_{RAD23}-*FLAG-rad23*^{uba} *TRP1* 2μ	This study

[a]All plasmids contain the Ap^R sequence.

Preparation of yeast cell lysates

Approximately 0.1 ml of cell pellet was suspended in 0.4–0.5 ml Buffer A (50 mM HEPES, pH 7.5, 150 mM NaCl, 5 mM EDTA, 1% Triton X-100) containing protease

inhibitors (Complete; Roche Diagnostics), and lysed with glass beads (425–600 μm; Sigma), using a cell disruptor (FastPrep20, ThermoSavant). Extracts were adjusted to equal volume and concentration, and analyzed either by immunoprecipitation (IP), or directly by electrophoresis in a polyacrylamide gel after boiling for 3 min in SDS sample buffer.

Immuno- and affinity-purification

FLAG-tagged proteins were immunoprecipitated with anti-FLAG M2-agarose beads (Sigma Chemical Co., St Louis), while HA-tagged Rad4 was purified on protein-A agarose (IPA 300; Repligen). GST-fusion proteins were isolated on glutathione–Sepharose beads (Amersham Pharmacia). Proteins were resolved by SDS–PAGE, transferred to nitrocellulose (BioRad), and incubated with the primary antibody (at dilutions recommended by the manufacturer). The reactions were developed with a luminol-based chemiluminescent reagent (Perkin-Elmer). The following antibodies were purchased. Anti-HA (Y-11 polyclonal, Santa Cruz Biotechnology); anti-FLAG (HRP-conjugated monoclonal, Sigma); anti-β-galactosidase (monoclonal, Promega); anti-His_6 (monoclonal, BD Biosciences). We generated antibodies against Rad23, and obtained anti-Pab1 from C. Wilusz and S. Peltz (RWJMS).

Pulse-chase analysis

Fifty ml cultures of exponentially growing cells were pelleted and resuspended in 0.4 ml labeling buffer (50 mM sodium phosphate, pH 7.0, 2% glucose); 0.5 mCi of EXPRE^{35}S^{35}S protein labeling mix (Perkin-Elmer) was added and the suspension incubated at 30°C for 10 min. Cells were washed with 1 ml water and resuspended in 0.4 ml chase buffer (YPD-glucose media containing excess cold L-methionine and L-cysteine, and 0.5 mg/ml cycloheximide); 0.1 ml of the suspension was immediately withdrawn, and frozen in liquid nitrogen. The rest of the suspension was incubated at 30°C, and additional 0.1 ml aliquots were withdrawn at the indicated times, and frozen. Trichloroacetic acid precipitation and scintillation counting estimated incorporation of ^{35}S into acid insoluble proteins. Lysates containing equal ^{35}S c.p.m. were adjusted to equal volume and used for HA-immunoprecipitations.

UV survival assays

Cells were grown in YPD to mid-log phase (~10^7 cells/ml), washed with sterile water and resuspended at OD_{600nm} of 1. Serial 10-fold dilutions were spread on YPD plates, and irradiated at 1 J/s/m^2 of predominantly 254 nm UV light, using an American Ultraviolet Co. germicidal lamp. Following irradiation, the plates were wrapped with aluminum foil and incubated at 30°C until colonies appeared (typically after 2–4 days depending on the genetic background). The number of colonies was counted, and the average results from duplicate experiments were plotted.

RESULTS

Characterization of an integrated derivative of Rad4–HA

Rad23 has a modest stabilizing effect on the abundance of highly over-expressed Rad4–HA, following DNA damage (20). Simultaneous over-expression of Rad23 reduced multi-ubiquitination of Rad4–HA, suggesting that Rad23 might influence Rad4 stability. However, since high levels of Rad23 (*in vivo* and *in vitro*) interfered with the ubiquitination and de-ubiquitination of test proteins (11,32–34), we were concerned that subtle regulatory effects of Rad23 could be masked when either protein was over-expressed. To minimize this potential risk, we generated a chromosomal copy of Rad4 that was linked to the HA epitope. Protein extracts were prepared from yeast cells that harbored integrated Rad4–HA, or expressed Rad4–HA from a high-copy plasmid, and examined by immunoblotting. A band consistent with the size of Rad4–HA was detected only in cells that expressed the tagged derivative (Figure 1A; lane 1 and 3). The extracts were also

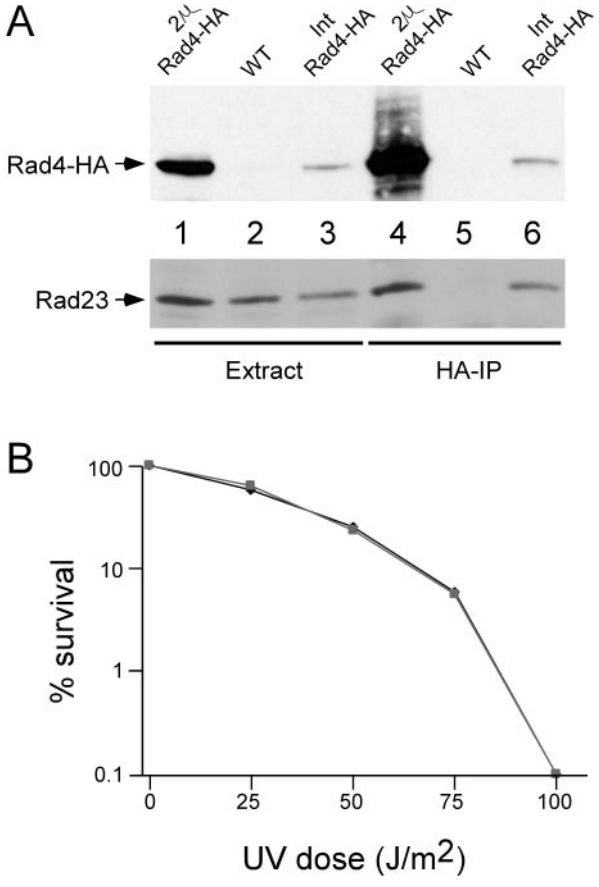

Figure 1. Physiological expression of an epitope-tagged derivative of Rad4. (**A**) The native *RAD4* gene was replaced with a version containing two tandem HA epitopes. Protein extracts were prepared and equal amounts were resolved by SDS–PAGE. A nitrocellulose filter was incubated with antibodies against HA and Rad4–HA was detected when expressed from a high copy plasmid (lane 1) and at physiological levels from the integrated gene (lane 3). Protein extracts were also incubated with anti-HA antibodies to immunoprecipitate Rad4–HA, and verify interaction with endogenous Rad23. High levels of Rad4–HA were recovered from cells expressing the protein from a high-copy plasmid, in contrast to ~25-fold lower levels from the integrated derivative. Rad23 was co-precipitated with Rad4–HA from both strains (lanes 4 and 6). Significantly, neither Rad4–HA nor Rad23 was purified from a strain that expressed untagged Rad4 (lane 5). (**B**) To confirm that Rad4–HA provided UV resistance, yeast cells were diluted to ~1×10^7/ml and spread evenly on agarose medium. The plates were exposed to 254 nm UV light for the doses indicated, covered with foil, and incubated at 30°C for ~3 days. The number of colonies was counted from duplicate experiments, and the average values are plotted. (Wild-type, gray square; Rad4–HA integrant, solid diamond.)

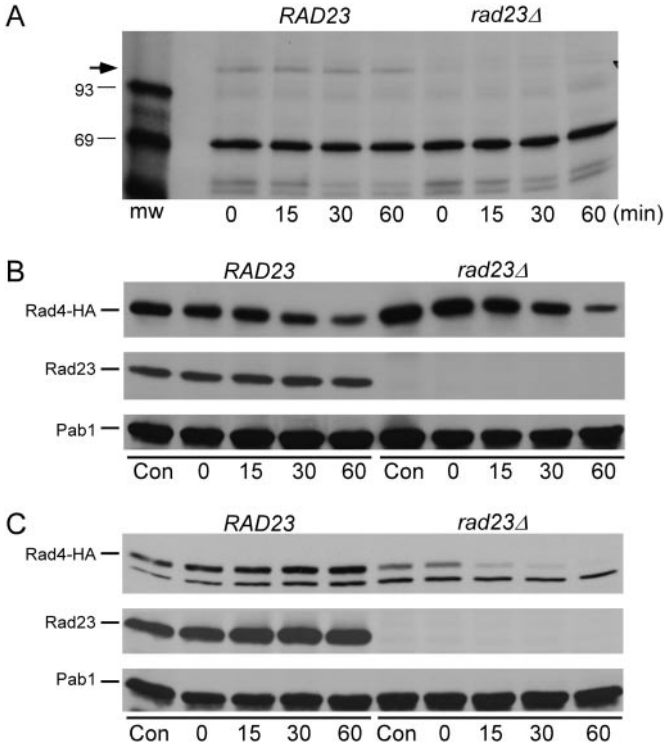

Figure 2. Rad23 regulates Rad4–HA abundance. (**A**) Wild-type and *rad23*Δ cells expressing physiological levels of Rad4–HA were incubated with ^{35}S-methionine + ^{35}S-cysteine for 10 min. The cells were suspended in medium containing excess unlabeled amino acids and cycloheximide. Extracts were prepared at the intervals indicated and Rad4–HA was immunoprecipitated (arrow) and detected by autoradiography. The major band at ~70 kDa is a non-specific interaction. The steady-state levels of Rad4–HA that was expressed from a high-copy plasmid (**B**) was compared to the expression from an integrated gene (**C**) in *RAD23* and *rad23*Δ cells. An aliquot was withdrawn from the culture before translation inhibitor was added (Con). Following addition of cycloheximide, aliquots were withdrawn immediately (0), and at the intervals indicated. Total protein was examined by SDS–PAGE and immunoblotting with anti-HA antibodies. Equality of protein loading was confirmed by incubating the same blot with antibodies against Pab1.

incubated with anti-HA antibodies and Rad4–HA was successfully immunoprecipitated when over-expressed (lane 4), and at much lower levels from the strain that expressed Rad4–HA at physiological levels (lane 6). As expected, incubation of an extract containing untagged Rad4 with anti-HA antibodies did not precipitate either Rad4 or Rad23 (lane 5). We estimated that Rad4–HA was expressed at ~25-fold higher levels from the plasmid (extract; compare lanes 1 and 3). We also determined that Rad23 could be co-purified with Rad4–HA (lanes 4 and 6, lower panel). At physiological levels, all cellular Rad4 is bound to Rad23. We therefore investigated if over-expression of Rad4 would lead to increased association with Rad23, which is expressed at much higher levels. Surprisingly, the amount of Rad23 that was co-precipitated with Rad4–HA was largely unaffected by its high-level expression (compare lanes 4 and 6; Figure 1A, lower panel), and it is possible that another limiting factor governs the formation and/or stability of the Rad23/Rad4 complex. It may be significant, therefore, that mammalian Rad23/Rad4 is associated with Centrin/Cdc31 protein (45), which can promote XPC stability in human cells. It is conceivable that Centrin/Cdc31 regulates the assembly of a Rad23/Rad4 complex. Furthermore, Rad23 is known to have many other cellular partners, and consequently most of it may be unavailable for interaction with Rad4. We also confirmed that Rad4–HA, expressed at physiological levels from the integrated locus, could functionally replace the native protein in NER (Figure 1B). The average value from duplicate measurements shows that integrated Rad4–HA is fully functional.

The stability of Rad4–HA is positively regulated by Rad23

To examine the role of Rad23 in controlling Rad4 stability, under physiological expression levels, we integrated Rad4–HA in *RAD23* and *rad23*Δ cells. To perform pulse-chase studies, actively growing cells were incubated with ^{35}S-methionine + ^{35}S-cysteine for 10 min, and chased in buffer containing unlabeled amino acids and cycloheximide. Aliquots of the labeled cells were withdrawn periodically and examined by immunoprecipitation (Figure 2A). A low level of an ~100 kDa protein was detected in *RAD23* (wild-type), but not in *rad23*Δ. Intriguingly, the low levels of ^{35}S-labeled Rad4–HA detected in *RAD23* was stable during the course of the 60 min chase, suggesting that a small fraction was safely incorporated into a complex containing Rad23 (25), and possibly Cdc31. A number of other ^{35}S-labeled proteins in the autoradiogram represent non-specific interaction with the affinity beads that were also detected in extracts lacking Rad4–HA, following long exposures to X-ray film.

To improve the detection of Rad4–HA, without requiring over-expression, we examined the steady-state levels of unlabeled Rad4–HA following inhibition of protein synthesis. Cycloheximide was added to actively growing yeast cells, and aliquots of the cultures were withdrawn and analyzed. Rad4–HA levels decreased moderately in both wild-type and *rad23*Δ cells, when Rad4–HA was over-expressed from a high-copy plasmid (Figure 2B; compare 0 and 60 min lanes). However, when Rad4–HA was expressed at physiological levels, its abundance was strongly dependent on the presence of Rad23 (Figure 2C), and a significant fraction was eliminated within 15 min. It is significant in this regard that 60 min after inhibition of protein synthesis, the steady-state level of over-expressed Rad4–HA exceeded the abundance of physiologically expressed Rad4–HA, even in the absence of protein synthesis inhibitor (compare Panel B *rad23*Δ 60 min, to Panel C *rad23*Δ Con). When expressed at physiological levels, Rad4–HA was eliminated by 30 min in *rad23*Δ (Figure 3A). It is likely that Rad4–HA is targeted for degradation soon after synthesis, because the levels present at 0 min was noticeably reduced in *rad23*Δ, compared to *RAD23*. The immunoblot was also incubated with antibodies against Pab1, to confirm equal loading of protein extracts (panels B and C). These results, which show that Rad23 can stabilize Rad4–HA, are strongly contrasted by its well-described role in promoting degradation of ubiquitinated proteins.

Plasmid-based Rad23 can restore Rad4–HA levels and efficient NER in *rad23*Δ

To extend these results *rad23*Δ and a congenic wild-type strain containing integrated Rad–HA were transformed with a plasmid encoding FLAG–Rad23. Yeast cells were grown to

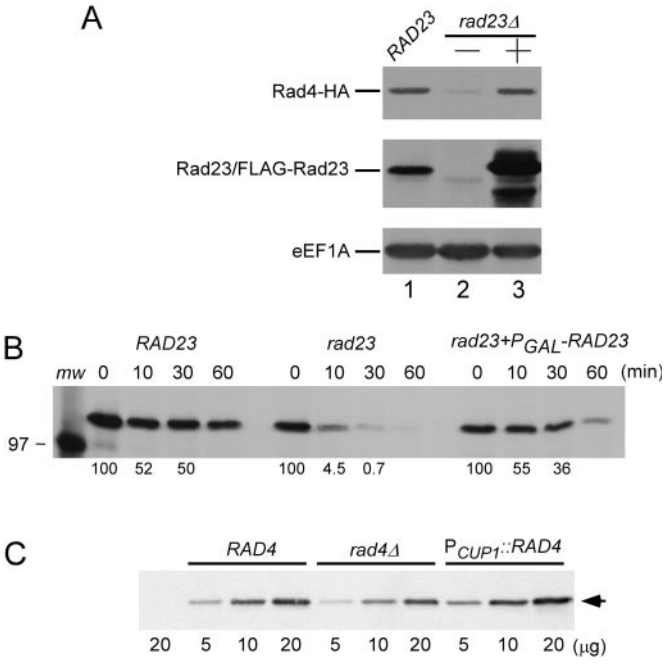

Figure 3. Episomal Rad23 can restore Rad4 levels in *rad23*Δ cells. (**A**) A plasmid encoding FLAG–Rad23 was transformed into wild-type and *rad23*Δ cells that also contained integrated Rad4–HA. The levels of Rad4–HA was determined by immunoblotting. Rad4–HA levels were restored to wild-type levels following transformation of the Rad23-encoding plasmid (compare lanes 1 and 3). FLAG–Rad23 is slightly larger than the native protein, and this difference is observed in SDS–PAGE. To confirm equality of loading, the same filters were incubated with antibodies against eEF1A. (**B**) The stability of Rad4–HA, expressed at high levels from a P_{CUP1}-driven promoter, was examined by pulse-labeling methods in cells containing or lacking Rad23. Aliquots of the labeled extracts were withdrawn at the times indicated, precipitated with anti-HA antibodies, and following SDS–PAGE, examined by autoradiography. The amount of Rad4–HA remaining over time is indicated at the bottom of the panel. (**C**) The levels of endogenous Rad23 were examined in yeast cells that expressed different levels of untagged Rad4. Three different loadings of total protein extract (5, 10 and 20 μg) were prepared from *RAD4*, *rad4*Δ and P_{CUP1}::*RAD4*-over-expressing cells and resolved by SDS–PAGE. An immunoblot was incubated with antibodies against Rad23.

exponential phase and protein extracts were resolved by SDS–PAGE and examined by immunoblotting. To confirm equality of loading, the filter was incubated with antibodies against eEF1A, and similar levels were detected in all the lanes (Figure 3A). Although the abundance of Rad4–HA was diminished significantly in *rad23*Δ (lane 2), co-expression of FLAG–Rad23 in *rad23*Δ (lane 3) restored Rad4–HA levels to that present in wild-type cells (lane 1), confirming that the stabilizing effect is dependent on the availability of Rad23.

To extend these findings, we examined the stability of Rad4–HA by pulse labeling. However, due to the difficulty of labeling the integrated derivative of Rad4–HA (Figure 2A), we examined the stability of an over-expressed derivative. Yeast cells were labeled with ^{35}S-methionine plus ^{35}S-cysteine for 5 min, and chased in medium containing excess unlabeled amino acids and cycloheximide. Equal amounts of trichloroacetic (TCA)-insoluble c.p.m. were incubated with antibodies against the HA epitope. Rad4–HA levels were measured in wild-type (*RAD23*), *rad23*Δ and *rad23*Δ cells, expressing native Rad23 from the galactose-inducible P_{GAL1} promoter. (All three cultures were grown in galactose-containing medium.) Autoradiographic exposures showed that the rapid degradation of Rad4–HA in *rad23*Δ was suppressed in the presence of Rad23. The images were quantified by densitometry, and relative values are indicated below the panels. (The values for the 60 min time-points could not be determined reliably). We note that when Rad4–HA was expressed at high levels (Figure 2B), we did not observe a marked difference in its stability in wild-type and *rad23*Δ cells. In contrast, the pulse-labeling studies (Figure 3B) indicate that newly synthesized Rad4 might be particularly susceptible to proteolysis. The fraction that escapes degradation could be stabilized through an interaction with physiological partners.

Both Rad4 and Rad23 were reported to be targets of the Ub/proteasome system (5,20,23–25,46). Although Rad23 is a stable protein (13), we questioned if its levels would be altered by high-level expression of Rad4–HA. We examined the steady-state levels of endogenous Rad23, using different amounts of protein extracts prepared from wild-type, *rad4*Δ and *rad4*Δ over-expressing Rad4 (Figure 3C). We determined that ~25-fold over-expression of Rad4 had no effect on the levels of Rad23. This is not unexpected because Rad23 is normally present at much higher levels than Rad4. Furthermore, we noted earlier that over-expression of Rad4–HA did not yield increased amounts of the dimer (Figure 1A), suggesting that the association could be regulated.

Rad4–HA is stabilized in proteasome mutants

UbL–UBA proteins, such as Rad23, perform a central role in the degradation of ubiquitinated proteins by the proteasome. Two distinct models have been proposed to describe the activity of Rad23. On the one hand, Rad23 might operate as a shuttle-factor that can bind and translocate ubiquitinated proteins to the proteasome (16). An alternative model envisions that Rad23 functions as a receptor in the proteasome (4). Given the close coupling of the activities of Rad23 with the proteasome, and the previously described requirement for the proteasome in NER, we examined Rad4–HA stability in proteasome mutants that lacked Rad23. We hypothesized that if Rad4–HA was destabilized in *rad23*Δ, a mutation in the proteasome might restore normal levels. Therefore, we integrated Rad4–HA in *sug1-20* and *sug1-25* mutants (15). Rpt6/Sug1 encodes an AAA-ATPase in the 19S regulatory particle (47). The *RAD23* gene was also deleted in these strains. Protein extracts were resolved by SDS–PAGE and higher levels of Rad4–HA were detected (Figure 4A), demonstrating that its degradation occurred through this proteolytic pathway. The autoradiographic exposures were quantified by densitometry, and relative values are shown. (These values were not standardized to the levels of Pab1, which is expressed at very high levels, because we were unable to obtain a linear response, even with reduced loading. We note, however, that the level of Pab1 in the *sug1-25* strain is lower than in the wild-type, suggesting that the levels of Rad4–HA are probably higher than indicated.) This result is consistent with a previous study in which over-expressed Rad4–HA was stabilized in an *rpt1* mutant, following DNA damage (20). Inhibition of the proteasome has also been reported to stabilize mXPC (23).

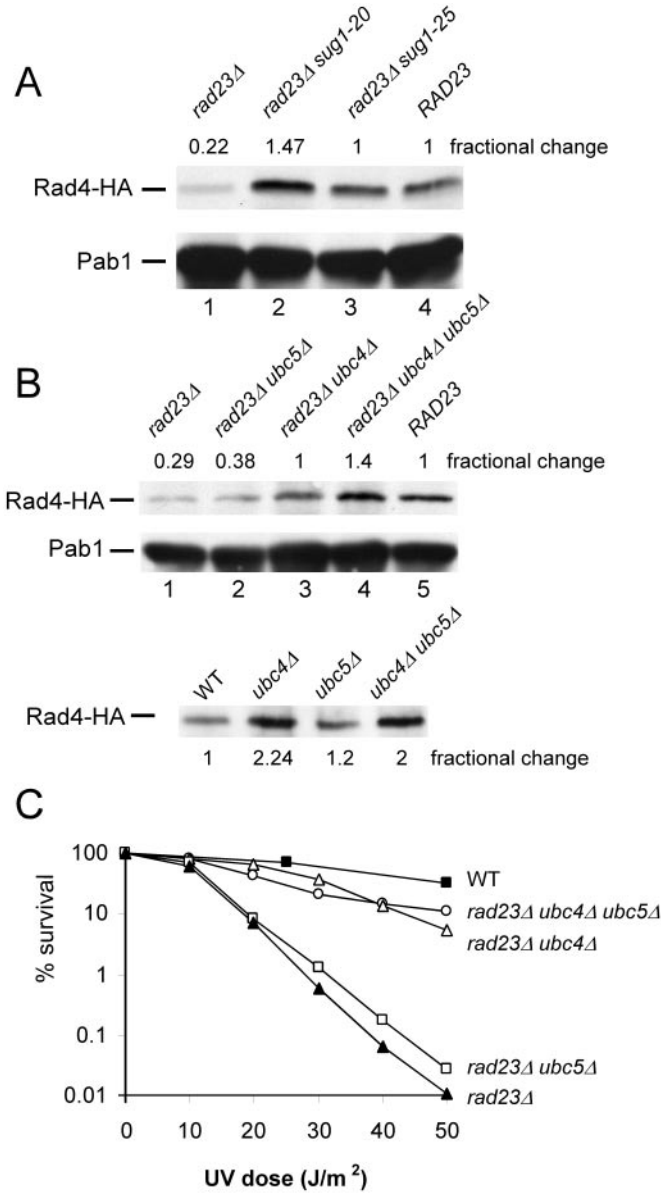

Figure 4. Rad4 levels are regulated by the Ub/proteasome system. (**A**) The levels of Rad4–HA were measured in the *sug1* proteasome mutant strain, and compared to wild-type and *rad23*Δ cells. The values above the panel indicate relative amounts of Rad4–HA that was measured by densitometry. (**B**) The decreased levels of Rad4–HA in *rad23*Δ are fully restored in a yeast mutant lacking the Ub-conjugating enzymes Ubc4 and Ubc5 (quantitation above the panel). The lower panel shows that Rad4–HA levels are also increased in a *RAD23* strain that lacks Ubc4 (or both Ubc4 and Ubc5; quantitation below the panel). (**C**) Yeast cells lacking Ubc4, or both Ubc4 and Ubc5, can strongly suppress the UV-sensitivity of *rad23*Δ. Although Ubc4 and Ubc5 are highly homologous, Ubc5 is expressed at very low levels, and primarily in growth-arrested cells. (Wild-type, solid square; *rad23*Δ, solid triangle; *rad23*Δ *ubc5*Δ, open square; *rad23*Δ *ubc4*Δ, open triangle; *rad23*Δ *ubc4*Δ *ubc5*Δ, open circle.)

The ubiquitin-conjugating enzymes, Ubc4 and Ubc5, promote Rad4 degradation

We reported previously that mutations in the Ub-fusion degradation (UFD) pathway partially suppressed the UV sensitivity of *rad23*Δ (48). The UFD system can recognize substrates that contain an N-terminal Ub extension (48). Intriguingly, Rad23 resembles a UFD substrate, and a recent study showed that Ufd2 could bind its UbL domain (19). However, the significance of this interaction is not known. Rad23 can also influence the stability of Ub–Pro–βgal, a well-characterized substrate of the UFD pathway. Despite these connections, the role of the UFD targeting system in NER is not known. Therefore, we investigated if targeting components of this pathway could affect the stability of Rad4, and contribute to the efficiency of DNA repair. We examined a set of mutant strains (49) to identify the Ub-conjugating enzyme that targeted Rad4, and detected significant stabilization in cells that lacked the closely related E2 enzymes Ubc4 and Ubc5 (50). These E2 enzymes play a central role in the UFD pathway. Consistent with the results in Figure 4A, Rad4–HA levels were significantly reduced in *rad23*Δ (Figure 4B, lane 1). However, Rad4–HA was stabilized in both *rad23*Δ *ubc4*Δ and *rad23*Δ *ubc4*Δ *ubc5*Δ strains (Figure 4B, lanes 3 and 4), but not in *rad23*Δ *ubc5*Δ. This finding is not unexpected, because Ubc5 is expressed at much lower levels than Ubc4. Ubc4 can fully compensate for the loss of Ubc5 (50). A recent study failed to detect significant stabilization of Rad4 in the *ubc4*Δ single mutant strain (24). It is possible that strain-specific effects account for these differences, since Ubc4/Ubc5 participate in a variety of cellular processes including cellular responses to pleiotropic stresses.

The stabilization of Rad4 in *ubc4*Δ *ubc5*Δ (Figure 4B) provides a logical explanation for the suppression of the UV sensitivity of *rad23*Δ (Figure 4C). Rad4–HA levels were even increased in single mutant strains that contained native Rad23 (Figure 4B, lower panel). Consistent with this model, we reported previously that over-expression of Ubc4 decreased UV resistance of wild-type cells (32). However, although Rad4–HA levels were restored, full suppression of the UV sensitivity of *rad23*Δ was not observed (Figure 4C). This result suggested that maintaining adequate levels of Rad4 represented only a subset of Rad23-specific activities in NER. It might be significant in this regard to consider the report by Friedberg and colleagues that Rad23/proteasome interaction was required for efficient NER, although it did not involve proteolysis (14,15). Collectively, these findings demonstrate that the availability of Rad4 has a strong bearing on the cellular tolerance to UV-induced DNA damage, but is in itself not sufficient for full NER.

A conserved motif in Rad23 (R4B) is sufficient for binding and stabilizing Rad4–HA

A short amino acid sequence in human Rad23 formed an interaction with XPC (39). Furthermore, the addition of this domain to a reconstituted reaction was sufficient for promoting XPC-dependent activity (39). We constructed a mutant of Rad23 that lacked a sequence resembling the motif in hHR23 that interacted with XPC. We generated a set of FLAG-tagged Rad23 mutants that lacked the N-terminal UbL domain, the putative Rad4-binding domain (ΔR4B), and a derivative in which both UBA domains were inactivated by single amino acid substitutions (16) (Figure 5A). These constructs were expressed in *rad23*Δ and their ability to suppress UV-sensitivity was assessed (Figure 5B). In agreement with previous studies (10), a *rad23* (uba$^-$) mutant that was unable to bind ubiquitinated proteins conferred normal

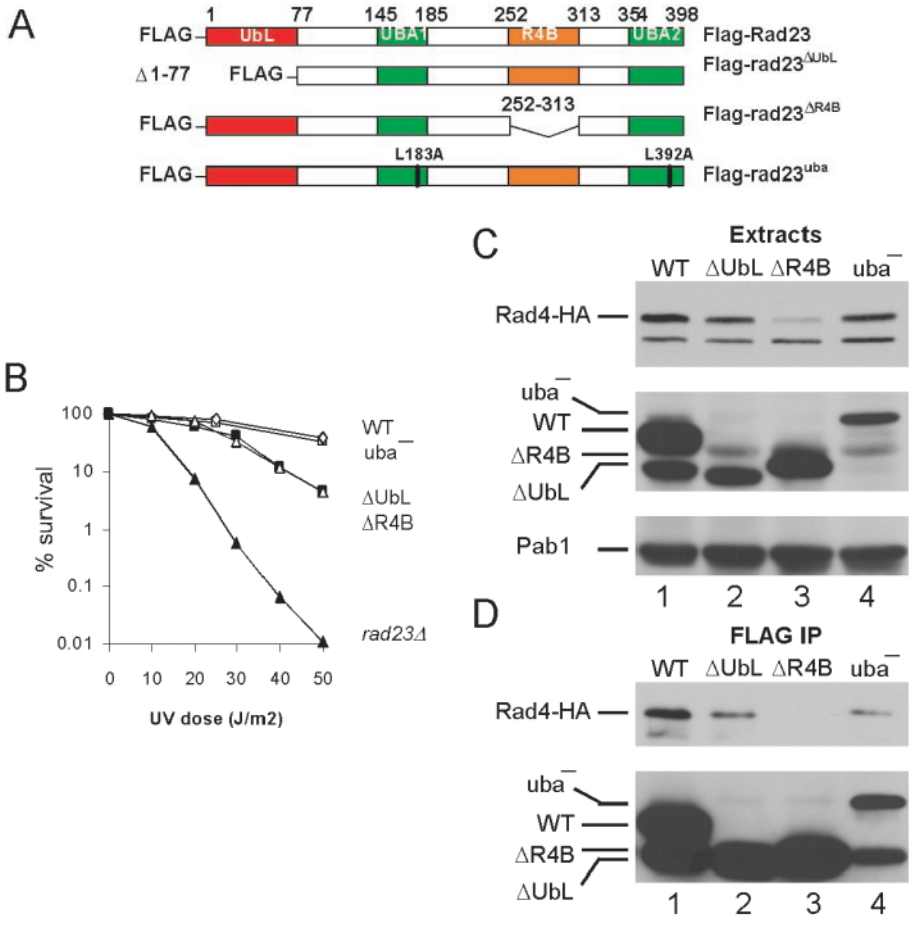

Figure 5. The Rad4-binding (R4B) domain in Rad23 is required for stabilizing Rad4–HA. (**A**) A scheme that indicates the various domains of Rad23 is shown. FLAG-tagged derivatives lacking the N-terminal UbL sequence, or the R4B sequence are shown. A derivative containing two single amino acid substitutions, in the two UBA domains, is also shown. (**B**) The DNA repair proficiency of each of the constructs described in (A) is shown. (Wild-type, open diamond; *rad23*Δ, solid triangle; *rad23*Δ + rad23$^{\Delta R4B}$ open triangle; *rad23*Δ + $^{\Delta UbL}$rad23, solid square; *rad23*Δ + rad23^{uba-}, open square). (**C**) The steady-state levels of Rad4–HA (expressed at physiological levels) are shown in yeast cells that expressed the various rad23 mutant proteins (described in A). Note the approximately equal expression of wild-type and rad23$^{\Delta R4B}$ proteins (lanes 1 and 3). Equality of loading was verified by probing the same filter with anti-Pab1 antibodies. (**D**) The interaction with Rad4–HA was specifically defective with rad23$^{\Delta R4B}$ protein (lane 3). The bars on the left indicate the approximate position of the various Rad23 proteins. Note, however, that $^{\Delta UbL}$rad23 and rad23$^{\Delta R4B}$ proteins migrated in the same position as the antibody heavy chain (~50 kDa). The FLAG–rad23^{uba-} mutant (uba^{-}) has a slower mobility in SDS–PAGE (lane 4), as noted previously (16). The faster migrating species in lane 1 represents a Rad23-specific degradation fragment.

resistance to UV light. However, the loss of either the UbL domain, or ΔR4B domain, resulted in reduced UV resistance, confirming the importance of both domains for conferring full resistance to DNA damage. Intriguingly, the intermediate level of UV-resistance observed in *rad23*Δ expressing either $^{\Delta UbL}$rad23 or rad23$^{\Delta R4B}$ was indistinguishable.

The steady-state abundance of Rad4–HA was determined in *rad23*Δ cells that expressed the set of FLAG-tagged Rad23 proteins (Figure 5C). We found that Rad4–HA levels were markedly reduced in cells that expressed rad23$^{\Delta R4B}$ (lane 3), suggesting that a failure to bind this rad23 mutant protein reduced Rad4 stability. To confirm this hypothesis, we immunoprecipitated the FLAG-tagged proteins and measured the co-purification of Rad4–HA (Figure 5D). As expected, an efficient interaction occurred with full-length Rad23 (WT; lane 1), and with mutants that either lacked the UbL domain (ΔUbL; lane 2), or contained defective UBA sequences (uba^{-}; lane 4). Significantly, rad23$^{\Delta R4B}$ did not bind Rad4–HA (compare lanes 1 and 3), confirming that similar sequences in yeast and human Rad23 proteins interact with Rad4/XPC, and impart stability. The reduced co-purification of Rad4–HA with $^{\Delta UbL}$rad23 (Figure 5D, lane 2) and rad23^{uba1,uba2} (Figure 5D, lane 4) probably reflects their lower expression, in comparison to full-length Rad23 (Figure 5C).

R4B is an autonomous sequence that can bind Rad4–HA and promote its stability

The XPC-binding domain of human Rad23 is sufficient for stimulating XPC-dependent excision activity (39). Based on these results, we investigated if the Rad4-binding domain (R4B) would be sufficient for stabilizing Rad4–HA in *rad23*Δ. The sequence encoding R4B was expressed in *RAD23* and *rad23*Δ cells as a fusion to glutathione *S*-transferase (GST–R4B), and Rad4–HA levels were measured in the presence of GST, GST–R4B and GST–Rad23 (Figure 6A; see lower panel for GST-fusion protein expression). In the wild-type strain (*RAD23*), similar levels of

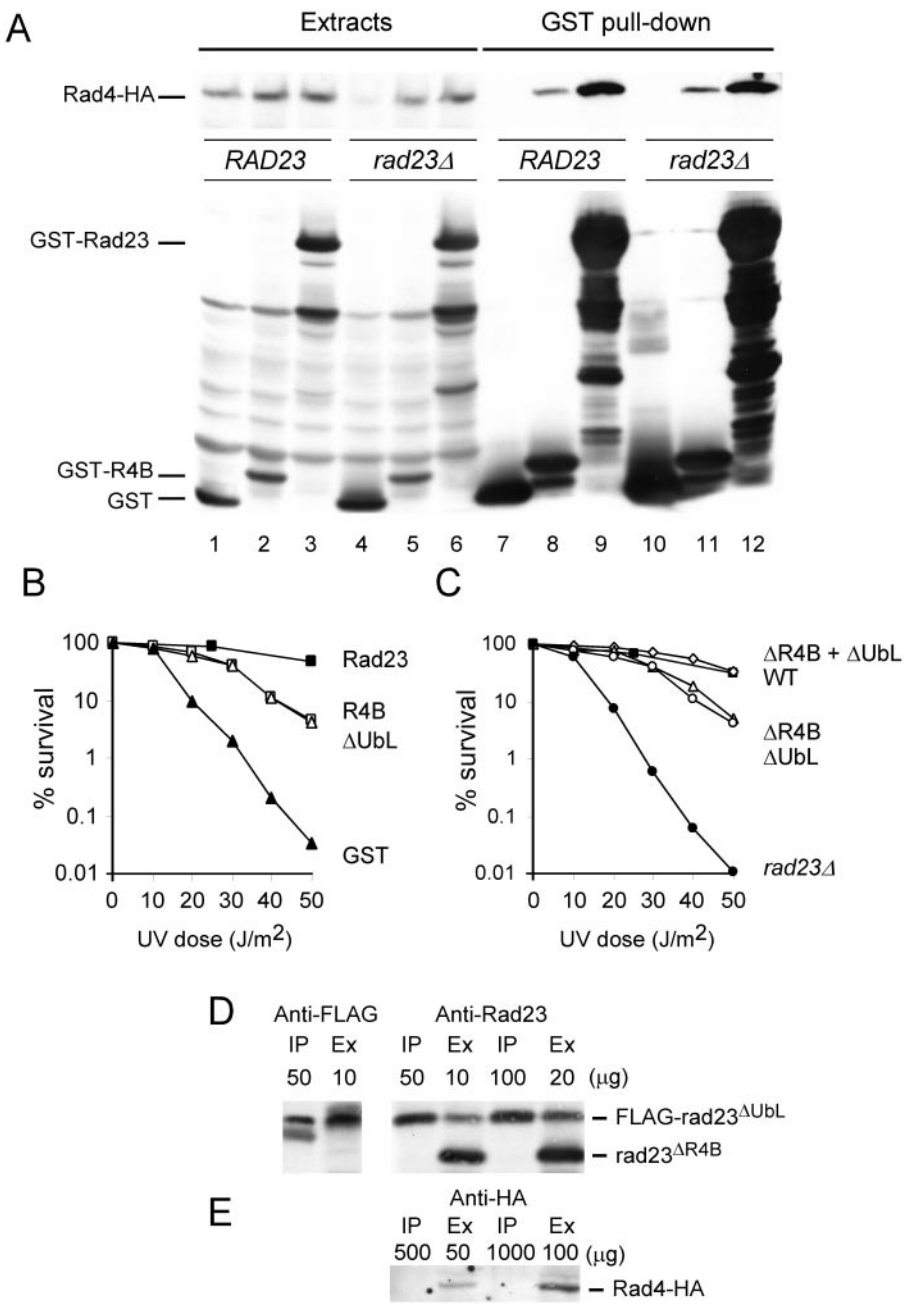

Figure 6. R4B is an autonomous Rad4-binding sequence that stabilizes Rad4, and restores significant UV resistance. (**A**) GST-fusion proteins (R4B or full-length Rad23) were expressed in yeast cells containing integrated Rad4–HA. Total extracts prepared from *RAD23* and *rad23*Δ cells were analyzed by SDS–PAGE, and an immunoblot incubated with antibodies against GST (Extracts). The positions of GST, GST–R4B and GST–Rad23 are indicated by the bars on the left of the lower panel. Equal amounts of extracts were incubated with glutathione–Sepharose to purify GST and the GST-fusion proteins (GST pull-down). Note the lower levels of GST–R4B in extracts and on the GST beads. The same reactions were also tested for the presence of Rad4–HA (upper panel). Expression of GST–R4B restored normal levels of Rad4–HA in the extracts (lane 5). Furthermore, affinity-purified GST–R4B was associated with Rad4–HA at comparable levels as the full-length GST–Rad23 protein (compare lanes 8, 9 and 11, 12). The relatively lower levels of Rad4–HA in lanes 8 and 11 reflect the lower expression of the GST–R4B construct (see lower panel). (**B**) The ability of GST–R4B to bind Rad4-HA led us to examine its capacity to suppress the UV-sensitivity of *rad23*Δ. Both rad23$^{\Delta R4B}$ and $^{\Delta UbL}$rad23 conferred an intermediate level of resistance. Wild-type, solid square; *rad23*Δ + GST, solid triangle; *rad23*Δ + GST–$^{\Delta UbL}$rad23, open triangle; *rad23*Δ + GST-rad23$^{\Delta R4B}$, open square. (**C**) To determine if rad23$^{\Delta R4B}$ and $^{\Delta UbL}$rad23 functioned in distinct pathways, both proteins were simultaneously expressed in *rad23*Δ cells containing integrated Rad4–HA. Complete suppression of the UV-sensitivity of *rad23*Δ was detected. (Wild-type, solid square; *rad23*Δ, solid circle; *rad23*Δ + GST–$^{\Delta UbL}$rad23, open circle; *rad23*Δ + GST–rad23$^{\Delta R4B}$, open triangle; *rad23*Δ + GST–$^{\Delta UbL}$rad23 + GST–rad23$^{\Delta R4B}$, open diamond.) (**D**) Plasmids expressing $^{\Delta UbL}$rad23 and FLAG–rad23$^{\Delta R4B}$ were transformed into cells expressing physiological levels of Rad4–HA. Protein extracts were prepared and incubated with antibodies against FLAG. The purified FLAG-rad23$^{\Delta UbL}$ protein is shown in the left panel (lower band is antibody heavy chain). We examined 10 μg of total protein to detect FLAG-rad23$^{\Delta UbL}$, applied 50 μg of total protein to recover FLAG-rad23$^{\Delta UbL}$ by immunoprecipitation. Immunoblots containing similar immunoprecipitation reactions were probed with antibodies against Rad23, so that both $^{\Delta UbL}$rad23 and FLAG–rad23$^{\Delta R4B}$ would be detected (right panel). As expected, both proteins were readily detected in the extract lanes (Ex). Significantly, we detected no evidence for $^{\Delta UbL}$rad23/FLAG–rad23$^{\Delta R4B}$ dimerization (see IP lanes). (We tested up to 1 mg of protein in the immunoprecipations, and did not detect an interaction.) (**E**) Immunoblots containing reactions with much larger quantity of protein extracts were reacted with antibodies against HA. We failed to detect Rad4–HA in association with FLAG–rad23$^{\Delta R4B}$, demonstrating the absence of dimerization.

Rad4–HA were detected in the presence of the various GST proteins (upper panel; lanes 1–3). As expected, Rad4–HA levels were reduced in *rad23*Δ (upper panel, GST; lane 4), but were completely restored by full-length Rad23 (GST–Rad23; lane 6). Remarkably, GST–R4B also promoted stabilization of Rad4–HA (lane 5). Rad4–HA levels were restored to wild-type levels, despite the lower expression of GST–R4B, compared to GST–Rad23 (see lanes 2 and 3; lower panel). To verify that the R4B domain restored Rad4–HA levels through direct binding, we applied extracts to glutathione–Sepharose and examined the bound proteins in an immunoblot (lanes 7–12). We detected Rad4–HA in association with both GST–Rad23 and GST–R4B, suggesting that the increased levels of Rad4–HA in *rad23*Δ cells were due to direct interaction with R4B. We note that although comparable levels of Rad4–HA were present in extracts from GST–Rad23 and GST–R4B expressing cells, more Rad4–HA was precipitated with full-length GST–Rad23 protein. This may be due to a weaker interaction between R4B and Rad4–HA.

Since GST–R4B stabilized Rad4 in *rad23*Δ, we tested its ability to provide resistance to UV light (Figure 6B). We determined that GST–R4B provided intermediate resistance, similar to mutants lacking R4B, or the UbL domain (Figure 5B). If the primary function of Rad23 were to stabilize Rad4, we would have expected to detect full suppression of the UV sensitivity of *rad23*Δ in cells expressing GST–R4B. However, this was not the case. Moreover, this scenario would not explain the requirement for UbL/proteasome interaction (5,13). The inability of stabilized Rad4 to fully suppress the UV sensitivity of *rad23*Δ indicated that other domains (in Rad23) were also required for providing full NER. We conclude that the stabilization of Rad4 represents only one of the NER-specific activities of Rad23; consistent with a previous study, which found that over-expression of Rad4 did not suppress the UV sensitivity of *rad23*Δ.

Evidence for dual functions for Rad23 in NER

Based on these findings, we questioned if the UbL domain, and the R4B sequence, participated in distinct activities in NER. We note that $^{\Delta UbL}$rad23 can bind Rad4 (Figure 5D), but not the proteasome (5), while rad23$^{\Delta R4B}$ interacts with the proteasome, but not Rad4 (Figure 5D). We co-transformed *rad23*Δ with plasmids expressing both $^{\Delta UbL}$rad23 and rad23$^{\Delta R4B}$. Remarkably, expression of both proteins restored UV resistance to wild-type levels (Figure 6C). This striking result supports the hypothesis that Rad23 participates in two independent activities during NER. Specifically, the stabilization of Rad4 defines one important function of Rad23, while UbL/proteasome binding contributes to a distinct activity that is unrelated to the stabilization of Rad4.

Previous studies suggested that Rad23 might dimerize. To discount the possibility that an interaction between $^{\Delta UbL}$rad23 and rad23$^{\Delta R4B}$ might restore Rad23 function, we co-expressed both proteins in yeast cells harboring an integrated copy of Rad4–HA. Yeast extracts were applied to FLAG–agarose and FLAG–rad23$^{\Delta R4B}$ was precipitated (Figure 6D). We incubated an immunoblot with antibodies against Rad23 and detected both $^{\Delta UbL}$rad23 and FLAG–rad23$^{\Delta R4B}$ in extracts. However, we detected no evidence for co-precipitation of $^{\Delta UbL}$rad23 with FLAG–rad23$^{\Delta R4B}$ (Figure 6D; IP lanes). Different amounts of protein extracts were examined and no evidence for binding was observed (even with 1 mg of protein). The immunoblots were subsequently reacted with antibodies against the HA epitope, and Rad4–HA was detected in the extracts, but was not purified with FLAG–rad23$^{\Delta R4B}$ (Figure 6E). These studies show that the co-expression of $^{\Delta UbL}$rad23 and FLAG–rad23$^{\Delta R4B}$ can restore full Rad23 function in NER, but this effect occurs through complementation in *trans*.

DISCUSSION

There is compelling evidence that Rad23 can promote proteolysis by the Ub/proteasome pathway. In contrast, Rad23 also performs an inhibitory function in NER. Rad23 interfered with the multi-ubiquitination of Rad4–HA (20), and the abundance of the mouse XPC protein was reduced in cells that lacked mHR23-B (21,23). Recent studies confirmed a role for Rad23, and other NER proteins, in regulating Rad4 (XPC) stability (24,25). We report that Rad23 participates in two distinct activities in NER. One of these functions of Rad23 involves stabilization of Rad4 through direct binding. In the absence of Rad23, Rad4 is rapidly degraded in a process that involves the Ubc4 and Ubc5 Ub-conjugating enzymes, and the proteasome (Lommel *et al*. and Figure 4). However, high-level expression of Rad4 only partially suppressed the UV sensitivity of *rad23* cells (C. Schauber and K. Madura, unpublished data), indicating that Rad23 is required, even if Rad4 is stabilized. An alternate pathway involving Rad7 and Rad16 (NEF4) also regulates Rad4 levels (24). A second function for Rad23 involves proteasome interaction. Previous studies showed that the proteasome could negatively regulate NER (15,20,32). Rad23 mediates two distinct effects in NER that involve proteasome interaction by the UbL domain, and stabilization of Rad4. Optimal NER requires both Rad23/proteasome and Rad23/Rad4 interaction, although these activities are separable.

The formation of the Rad4/Rad23 dimer promotes Rad4 stability, and might be induced following DNA damage. A previous study characterized the activity of the XPC-binding peptide in a reconstituted system and observed that it stimulated XPC-dependent DNA incision (39). We show that the corresponding sequence in yeast Rad23 not only stimulated NER activity, but also protected Rad4 from degradation. In contrast, Rad23/proteasome interaction during NER promotes a different function that does not involve Rad4. Therefore, the previously described non-proteolytic function of Rad23 in NER (14,15) is distinct from its role as a facilitator of protein degradation by the Ub/proteasome system.

The dual function of Rad23 in NER is an important finding. On the one hand, we show that Rad23 can bind Rad4 through a dedicated sequence (R4B). This interaction stabilizes Rad4, and a failure causes UV-sensitivity. Although a low level of Rad4–HA was detected in *rad23*Δ cells expressing FLAG–rad23$^{\Delta R4B}$, we did not observe an interaction. Consequently, the inability of FLAG–rad23$^{\Delta R4B}$ to bind Rad4 results in significantly reduced levels, and an NER defect. However, if this were the sole NER function of Rad23, we would expect FLAG–rad23$^{\Delta R4B}$ to be as sensitive to UV light as *rad23*Δ. Clearly, this was not the case, as the FLAG–rad23$^{\Delta R4B}$ mutant provided an intermediate level of resistance (Figure 5B).

In contrast, $^{\Delta UbL}$rad23 is unable to interact with the proteasome, although it can bind Rad4. This mutant also provided an intermediate level of resistance to UV light, although ample Rad4–HA was available. Thus, both proteasome binding and Rad4 stabilization by Rad23 are required for efficient NER. That these are separable functions became evident when we discovered that full resistance to UV light was restored when rad23$^{\Delta R4B}$ and $^{\Delta UbL}$rad23 were co-expressed in *rad23*Δ. Complementation in *trans* shows that the two mutant proteins are competent in independent activities. The possibility that rad23$^{\Delta R4B}$ might dimerize with $^{\Delta UbL}$rad23 to confer Rad23 activity is considered unlikely, as we did not detect any evidence for an interaction.

Gillette *et al*. found that *sug1* and *sug2* mutants could restore partial NER in *rad23*Δ, to a level that is observed in cells expressing $^{\Delta UbL}$rad23. Rad4–HA levels are increased in this strain (Figure 4A). However, the *sug1* and *sug2* mutants did not improve NER in a *rad23*Δ mutant that expressed $^{\Delta UbL}$rad23. We note that $^{\Delta UbL}$rad23 cannot bind the proteasome, but can bind and stabilize Rad4, and provide moderate levels of NER. These data are consistent with our evidence that both proteasome interaction and Rad4-stabilization by Rad23 are required for complete UV resistance. Furthermore, mutations in the catalytic core particle did not mirror the results in *sug1* and *sug2*, suggesting that efficient NER might involve two actions of Rad23, one of which is non-proteolytic. The non-proteolytic role of the proteasome is poorly defined. It is possible that the proteasome contributes to chromatin remodeling or recycling of NER complexes (20).

In an attempt to characterize the mechanism of targeting, we examined Rad4–HA levels in strains harboring mutations in ubiquitin-conjugating enzymes. We identified Ubc4 and Ubc5 as the E2 enzymes that contributed to the degradation of Rad4. Ubc4 and Ubc5 are redundant enzymes, although Ubc4 is predominant due to its higher level of expression. A double mutant (*ubc4*Δ *ubc5*Δ) is sensitive to environmental stresses, and is severely defective in degradation of bulk proteins, as well as certain test proteins (50). We showed previously that over-expression of Ubc4 increased UV sensitivity moderately (32), although the underlying mechanism was not determined. Based on the results described here, we believe that high-level expression of Ubc4 increases the degradation of Rad4. In agreement with this model, Rad4–HA was stabilized in *rad23*Δ *ubc4*Δ *ubc5*Δ, and intermediate UV resistance was detected.

The effect of Rad23 is redundant with NEF4, demonstrating that multiple pathways affect Rad4 levels. However, the strong stabilization of Rad4 in *rad7*Δ and *rad16*Δ was not accompanied by UV resistance, suggesting that NEF4 has other DNA damage-specific targets, whose degradation promotes repair (24). In contrast, Rad4 levels were significantly reduced in *rad23*Δ *rad7*Δ, and these cells are much more sensitive to UV-light than the single mutant strains. These results partly resolve the debate concerning the role of the Ub/proteasome system in DNA repair, and in particular, the conflicting role of Rad23 in having both positive and negative functions. The stabilization of Rad4 by Rad23 is an unusual role, since Rad23 is known primarily for its ability to promote degradation by the Ub/proteasome pathway. These findings therefore add a new dimension to the well-described properties of this highly conserved protein.

ACKNOWLEDGEMENTS

We thank members of the laboratory for comments on the manuscript. We thank R. D. Gietz (Univ. Manitoba, Canada) for plasmids, and C. Wilusz and S. Peltz (RWJMS) for antibodies against Pab1. We are grateful to Dr E. Friedberg for providing *sug1* mutant strains. We thank K. Sugasawa for sharing unpublished studies. This work was supported by Public Health Service grant CA-80835 from the National Cancer Institute.

REFERENCES

1. Batty,D.P. and Wood,R.D. (2000) Damage recognition in nucleotide excision repair of DNA2. *Gene*, **241**, 193–204.
2. Prakash,S. and Prakash,L. (2000) Nucleotide excision repair in yeast. *Mutat. Res*., **451**, 13–24.
3. Lambertson,D., Chen,L. and Madura,K. (1999) Pleiotropic defects caused by loss of the proteasome-interacting factors Rad23 and Rpn10 of *Saccharomyces cerevisiae*. *Genetics*, **153**, 69–79.
4. Elsasser,S., Chandler-Militello,D., Muller,B., Hanna,J. and Finley,D. (2004) Rad23 and Rpn10 serve as alternative ubiquitin receptors for the proteasome. *J. Biol. Chem*., **279**, 26817–26822.
5. Schauber,C., Chen,L., Tongaonkar,P., Vega,I., Lambertson,D., Potts,W. and Madura,K. (1998) Rad23 links DNA repair to the ubiquitin/proteasome pathway. *Nature*, **391**, 715–718.
6. Elsasser,S., Galim,R.R., Schwickart,M., Larsen,C.N., Leggett,D.S., Muller,B., Feng,M.T., Tubing,F., Dittmar,G.A. and Finley,D. (2002) Proteasome subunit Rpn1 binds ubiquitin-like protein domains. *Nature Cell Biol*., **4**, 725–730.
7. Funakoshi,M., Sasaki,T., Nishimoto,T. and Kobayashi,H. (2002) Budding yeast Dsk2p is a polyubiquitin-binding protein that can interact with the proteasome. *Proc. Natl Acad. Sci. USA*, **99**, 745–750.
8. Hiyama,H., Yokoi,M., Masutani,C., Sugasawa,K., Maekawa,T., Tanaka,K., Hoeijmakers,J.H. and Hanaoka,F. (1999) Interaction of hHR23 with S5a. The ubiquitin-like domain of hHR23 mediates interaction with S5a subunit of 26 S proteasome. *J. Biol. Chem*., **274**, 28019–28025.
9. Hofmann,K. and Bucher,P. (1996) The UBA domain: a sequence motif present in multiple enzyme classes of the ubiquitination pathway. *Trends Biochem. Sci*., **21**, 172–173.
10. Bertolaet,B.L., Clarke,D.J., Wolff,M., Watson,M.H., Henze,M., Divita,G. and Reed,S.I. (2001) UBA domains of DNA damage-inducible proteins interact with ubiquitin. *Nature Struct. Biol*., **8**, 417–422.
11. Chen,L., Shinde,U., Ortolan,T.G. and Madura,K. (2001) Ubiquitin-associated (UBA) domains in Rad23 bind ubiquitin and promote inhibition of multi-ubiquitin chain assembly. *EMBO Rep*., **2**, 933–938.
12. Wilkinson,C.R., Seeger,M., Hartmann-Petersen,R., Stone,M., Wallace,M., Semple,C. and Gordon,C. (2001) Proteins containing the UBA domain are able to bind to multi-ubiquitin chains. *Nature Cell Biol*., **3**, 939–943.
13. Watkins,J.F., Sung,P., Prakash,L. and Prakash,S. (1993) The *Saccharomyces cerevisiae* DNA repair gene RAD23 encodes a nuclear protein containing a ubiquitin-like domain required for biological function. *Mol. Cell. Biol*., **13**, 7757–7765.
14. Russell,S.J., Reed,S.H., Huang,W., Friedberg,E.C. and Johnston,S.A. (1999) The 19S regulatory complex of the proteasome functions independently of proteolysis in nucleotide excision repair. *Mol. Cell*, **3**, 687–695.
15. Gillette,T.G., Huang,W., Russell,S.J., Reed,S.H., Johnston,S.A. and Friedberg,E.C. (2001) The 19S complex of the proteasome regulates nucleotide excision repair in yeast. *Genes Dev*., **15**, 1528–1539.
16. Chen,L. and Madura,K. (2002) Rad23 promotes the targeting of proteolytic substrates to the proteasome. *Mol. Cell. Biol*., **22**, 4902–4913.
17. Saeki,Y., Saitoh,A., Toh-e,A. and Yokosawa,H. (2002) Ubiquitin-like proteins and Rpn10 play cooperative roles in ubiquitin-dependent proteolysis. *Biochem. Biophys. Res. Commun*., **293**, 986–992.
18. Verma,R., Oania,R., Graumann,J. and Deshaies,R.J. (2004) Multiubiquitin chain receptors define a layer of substrate selectivity in the ubiquitin-proteasome system. *Cell*, **118**, 99–110.

19. Kim,I., Mi,K. and Rao,H. (2004) Multiple interactions of rad23 suggest a mechanism for ubiquitylated substrate delivery important in proteolysis. *Mol. Biol. Cell*, **15**, 3357–3365.
20. Lommel,L., Ortolan,T., Chen,L., Madura,K. and Sweder,K.S. (2002) Proteolysis of a nucleotide excision repair protein by the 26 S proteasome. *Curr. Genet.*, **42**, 9–20.
21. Ng,J.M., Vrieling,H., Sugasawa,K., Ooms,M.P., Grootegoed,J.A., Vreeburg,J.T., Visser,P., Beems,R.B., Gorgels,T.G., Hanaoka,F., Hoeijmakers,J.H. and van der Horst,G.T. (2002) Developmental defects and male sterility in mice lacking the ubiquitin-like DNA repair gene mHR23B. *Mol. Cell. Biol.*, **22**, 1233–1245.
22. Sweder,K. and Madura,K. (2002) Regulation of repair by the 26S proteasome. *J. Biomed. Biotechnol.*, **2**, 94–105.
23. Ng,J.M., Vermeulen,W., van der Horst,G.T., Bergink,S., Sugasawa,K., Vrieling,H. and Hoeijmakers,J.H. (2003) A novel regulation mechanism of DNA repair by damage-induced and RAD23-dependent stabilization of xeroderma pigmentosum group C protein. *Genes Dev.*, **17**, 1630–1645.
24. Ramsey,K.L., Smith,J.J., Dasgupta,A., Maqani,N., Grant,P. and Auble,D.T. (2004) The NEF4 complex regulates Rad4 levels and utilizes Snf2/Swi2-related ATPase activity for nucleotide excision repair. *Mol. Cell. Biol.*, **24**, 6362–6378.
25. Okuda,Y., Nishi,R., Ng,J.M., Vermeulen,W., van der Horst,G.T., Mori,T., Hoeijmakers,J.H., Hanaoka,F. and Sugasawa,K. (2004) Relative levels of the two mammalian Rad23 homologs determine composition and stability of the xeroderma pigmentosum group C protein complex. *DNA Repair* (*Amsterdam*), **3**, 1285–1295.
26. Masutani,C., Sugasawa,K., Yanagisawa,J., Sonoyama,T., Ui,M., Enomoto,T., Takio,K., Tanaka,K., van der Spek,P.J., Bootsma,D. *et al.* (1994) Purification and cloning of a nucleotide excision repair complex involving the xeroderma pigmentosum group C protein and a human homologue of yeast RAD *EMBO J.*, **13**, 1831–1843.
27. Guzder,S.N., Sung,P., Prakash,L. and Prakash,S. (1995) Reconstitution of yeast nucleotide excision repair with purified Rad proteins, replication protein A, and transcription factor TFIIH. *J. Biol. Chem.*, **270**, 12973–12976.
28. Guzder,S.N., Sung,P., Prakash,L. and Prakash,S. (1998) Affinity of yeast nucleotide excision repair factor 2, consisting of the Rad4 and Rad23 proteins, for ultraviolet damaged DNA. *J. Biol. Chem.*, **273**, 31541–31546.
29. Jansen,L.E., Verhage,R.A. and Brouwer,J. (1998) Preferential binding of yeast RadRad23 complex to damaged DNA. *J. Biol. Chem.*, **273**, 33111–33114.
30. Guzder,S.N., Sung,P., Prakash,L. and Prakash,S. (1999) Synergistic interaction between yeast nucleotide excision repair factors NEF2 and NEF4 in the binding of ultraviolet-damaged DNA. *J. Biol. Chem.*, **274**, 24257–24262.
31. Hey,T., Lipps,G., Sugasawa,K., Iwai,S., Hanaoka,F. and Krauss,G. (2002) The XPC-HR23B complex displays high affinity and specificity for damaged DNA in a true-equilibrium fluorescence assay. *Biochemistry*, **41**, 6583–6587.
32. Ortolan,T.G., Tongaonkar,P., Lambertson,D., Chen,L., Schauber,C. and Madura,K. (2000) The DNA repair protein rad23 is a negative regulator of multi-ubiquitin chain assembly. *Nature Cell Biol.*, **2**, 601–608.
33. Raasi,S. and Pickart,C.M. (2003) Rad23 ubiquitin-associated domains (UBA) inhibit 26 S proteasome-catalyzed proteolysis by sequestering lysine 48-linked polyubiquitin chains. *J. Biol. Chem.*, **278**, 8951–8959.
34. Hartmann-Petersen,R., Hendil,K.B. and Gordon,C. (2003) Ubiquitin binding proteins protect ubiquitin conjugates from disassembly. *FEBS Lett.*, **535**, 77–81.
35. Johnson,P.R., Swanson,R., Rakhilina,L. and Hochstrasser,M. (1998) Degradation signal masking by heterodimerization of MATalpha2 and MATa1 blocks their mutual destruction by the ubiquitin-proteasome pathway. *Cell*, **94**, 217–227.
36. Clarke,D.J., Mondesert,G., Segal,M., Bertolaet,B.L., Jensen,S., Wolff,M., Henze,M. and Reed,S.I. (2001) Dosage suppressors of pds1 implicate ubiquitin-associated domains in checkpoint control. *Mol. Cell. Biol.*, **21**, 1997–2007.
37. Perozzi,G. and Prakash,S. (1986) RAD7 gene of *Saccharomyces cerevisiae*: transcripts, nucleotide sequence analysis, and functional relationship between the RAD7 and RAD23 gene products. *Mol. Cell. Biol.*, **6**, 1497–1507.
38. Wang,Z., Wei,S., Reed,S.H., Wu,X., Svejstrup,J.Q., Feaver,W.J., Kornberg,R.D. and Friedberg,E.C. (1997) The RAD7, RAD16, and RAD23 genes of *Saccharomyces cerevisiae*: requirement for transcription-independent nucleotide excision repair *in vitro* and interactions between the gene products. *Mol. Cell. Biol.*, **17**, 635–643.
39. Masutani,C., Araki,M., Sugasawa,K., van der Spek,P.J., Yamada,A., Uchida,A., Maekawa,T., Bootsma,D., Hoeijmakers,J.H. and Hanaoka,F. (1997) Identification and characterization of XPC-binding domain of hHR23B. *Mol. Cell. Biol.*, **17**, 6915–6923.
40. Sugasawa,K., Masutani,C., Uchida,A., Maekawa,T., van der Spek,P.J., Bootsma,D., Hoeijmakers,J.H. and Hanaoka,F. (1996) HHR23B, a human Rad23 homolog, stimulates XPC protein in nucleotide excision repair *in vitro*. *Mol. Cell. Biol.*, **16**, 4852–4861.
41. Rothstein,R. (1991) Targeting, disruption, replacement, and allele rescue: integrative DNA transformation in yeast. *Methods Enzymol.*, **194**, 281–301.
42. Gietz,R.D. and Prakash,S. (1988) Cloning and nucleotide sequence analysis of the *Saccharomyces cerevisiae* RAD4 gene required for excision repair of UV-damaged DNA. *Gene*, **74**, 535–541.
43. Gietz,R.D. and Sugino,A. (1988) New yeast–*Escherichia coli* shuttle vectors constructed with *in vitro* mutagenized yeast genes lacking six-base pair restriction sites. *Gene*, **74**, 527–534.
44. Baniahmad,C., Baniahmad,A. and O'Malley,B.W. (1994) A rapid method combining a functional test of fusion proteins *in vivo* and their purification. *Biotechniques*, **16**, 194–196.
45. Araki,M., Masutani,C., Takemura,M., Uchida,A., Sugasawa,K., Kondoh,J., Ohkuma,Y. and Hanaoka,F. (2001) Centrosome protein centrin 2/caltractin 1 is part of the xeroderma pigmentosum group C complex that initiates global genome nucleotide excision repair. *J. Biol. Chem.*, **276**, 18665–18672.
46. Kumar,S., Talis,A.L. and Howley,P.M. (1999) Identification of HHR23A as a substrate for E6-associated protein-mediated ubiquitination. *J. Biol. Chem.*, **274**, 18785–18792.
47. Glickman,M.H., Rubin,D.M., Fried,V.A. and Finley,D. (1998) The regulatory particle of the *Saccharomyces cerevisiae* proteasome. *Mol. Cell. Biol.*, **18**, 3149–3162.
48. Johnson,E.S., Ma,P.C., Ota,I.M. and Varshavsky,A. (1995) A proteolytic pathway that recognizes ubiquitin as a degradation signal. *J. Biol. Chem.*, **270**, 17442–17456.
49. Chen,P., Johnson,P., Sommer,T., Jentsch,S. and Hochstrasser,M. (1993) Multiple ubiquitin-conjugating enzymes participate in the *in vivo* degradation of the yeast MATα2 repressor. *Cell*, **74**, 357–369.
50. Seufert,W. and Jentsch,S. (1990) Ubiquitin-conjugating enzymes UBC4 and UBC5 mediate selective degradation of short-lived and abnormal proteins. *EMBO J.*, **9**, 543–550.